# 3D Printing of Anisotropic Polymer Nanocomposites with Aligned $BaTiO_3$ Nanowires for Enhanced Energy Density

Hang Luo[a], Xuefan Zhou[a], Ru Guo[a], Xi Yuan[a]*, Hehao Chen[a], Kechao Zhou[a], Isaac Abrahams[b], Dou Zhang[a]*

[a] State Key Laboratory of Powder Metallurgy, Central South University, Changsha, Hunan 410083, China

[b] Materials Research Institute, School of Biological Sciences, Queen Mary University of London, Mile End Road, London E1 4NS, UK

The Email of the corresponding author:

dzhang@csu.edu.cn (D. Zhang)

yuanxi0731@163.com (X. Yuan)

**Abstract**

High power density capacitors possess broad application prospects in electric vehicles and power transmission systems. The development of capacitors with high energy density to achieve miniaturization and lightweight applications is the bottle-neck in this field. Strategies including orientated distribution of fillers have been utilized to increase the energy density of the dielectrics. In this work, we demonstrate high-performance flexible p(olyvinylidene fluoride-chlorotrifluoroethylene) (P(VDF-CTFE)) nanocomposites with aligned $BaTiO_3$ nanowires using 3D printing technology. The 3D printing process is computer-controlled, which can effectively achieve designed geometric shapes and precise size. The resulting $BaTiO_3$ nanowires are highly aligned in a direction parallel to the surface of the nanocomposites due to the high shear environment within the very small 100 μm diameter nozzle. The highest energy density reached for these nanocomposites, with aligned $BaTiO_3$ nanowires, was 14.52 J $cm^{-3}$, which is 55% higher than that of nanocomposites with randomly aligned $BaTiO_3$ nanowires at the same loading level. This facile and readily scalable method of aligning one-dimensional fillers in a polymer matrix has potential not only in dielectric capacitor technology, but also in other fields where directional arrangement of low dimensional nanostructured materials is needed.

**Key words**: Alignment; 3D printing; $BaTiO_3$ nanowires; Dielectric composites

## 1 Introduction

High performance dielectric capacitors have been widely applied in electrical and electronic systems, such as electric vehicles, wind generators and aerospace power conditioning, due to their merits of super high power density and ability to withstand high operating voltage.[1-7] The dielectric materials used in commercially available capacitors are mainly based on biaxially oriented polypropylenes (BOPP), which exhibit energy densities of only 1~1.2 J $cm^{-3}$ at high applied electric field (~640 kV $mm^{-1}$).[8] In this case, the low energy density of the dielectric becomes a limitation to their application. [9-11] Generally, the discharge energy density ($J_{dis}$) of a capacitor is determined by the equation, $J_{dis} = \int_0^{D_{max}} EdD$, where $D$ and $E$ are applied electric field and the electric displacement, respectively.[12-14] For linear dielectrics, $J_{dis}$ can be evaluated by $J_{dis} = \frac{1}{2}\varepsilon_0\varepsilon_r E^2$, where $\varepsilon_0$ is the permittivity of free space and $\varepsilon_r$ is the relative permittivity. Therefore, the two key parameters for enhancing $J_{dis}$ are the relative permittivity and the largest applied electric field i.e. the breakdown strength ($E_b$).[15-17]

PVDF based nanocomposites with embedded ferroelectric ceramics such as $BaTiO_3$[18, 19], $Ba_{1-x}Sr_xTiO_3$[20], and $Pb(Zr_{1-x}Ti_x)O_3$[21] show enhanced energy density due to the combination of the high relative permittivity from the ferroelectric ceramics and high breakdown strength of the PVDF polymer matrix. In our previous work, ceramic fillers with high aspect ratios, such as $BaTiO_3$[22-24], $Na_{0.5}Bi_{0.5}TiO_3$[25], $TiO_2$@PZT[26, 27], and $Na_2Ti_3O_7$ nanowires [28] were employed to build dielectric capacitors with improved permittivity and energy density. The improvment in energy density is attributed

to the high breakdown strength mainatined by low ceramic loadings and increased relative permittivity due to the high aspect ratio fillers.[29]

In ceramic/polymer nanocomposites, electrons can move from one nanowire to another when the nanowires are randomly distributed due to multiple cross contacts between wires. This tunneling effect [30, 31] leads to lowering of breakdown strength. In contrast, if the ceramic nanowires are arranged in the polymer matrix in an orientated direction, e.g. perpendicular to the electric field, the electronic transmission pathway is blocked resulting in an enhanced breakdown strength.[32] Andrews et al. focused on finite element models to demonstrate that the orientation of the filler plays a critical role in achieving high dielectric and electromechanical coupling in the composites.[33] Exprimental work using different strategies, such as tape-casting[34], uniaxial strain[21], and electrospinning[35, 36] demonstrated that spatial distribution of the fillers also plays a large role in the dielectric and energy storage properties of the composites.

A major obstacle lies in developing an effective technique for aligning the one dimensional fillers in the polymer matrix. Three-dimensional printing (3D printing, also known as additive manufacturing) is widely regarded as a revolution in manufacturing technology, with significant promise for electronic applications.[37-39] During the printing process, the ceramic/polymer slurry experiences a high shear environment within the very small nozzle (typically with a diameter of 100 μm), which will produce high orientation of the fillers and form anisotropic materials.[39, 40] In addition, 3D printing is a computer-controlled technique, which can print

samples with designed geometric shape, precise size, short processing times and at low cost.[41, 42]

Here, we demonstrate high-performance flexible p(olyvinylidene fluoride-chlorotrifluoroethylene) (PVDF-CTFE) nanocomposites with aligned $BaTiO_3$ nanowires using 3D printing technology. $BaTiO_3$ nanowires were embedded and aligned in a P(VDF-CTFE) polymer matrix by tunable internal friction during the extrusion. The rheological properties of the $BaTiO_3$/P(VDF-CTFE) slurry with $BaTiO_3$ loadings that lead to the orientation during the 3D printing process were investigated. Significant performance enhancements, including breakdown strength and energy density improvements, were achieved compared with nanocomposites prepared by a casting method. We believe that 3D printing technology has great potential in the development of dielectric nanocomposites with controllable anisotropic properties for a broad range of applications.

## 2 Experimental section

### 2.1 Synthesis of $BaTiO_3$ nanowires

The $BaTiO_3$ nanowires were synthesized by a hydrothermal method according to previous work.[43] Firstly, 1.446 g of titanium oxide ($TiO_2$, anatase) was added to 70 ml NaOH solution (10 M) and the mixture was stirred for 2 h to form a homogeneous suspension. The hydrothermal reactions were carried out at 210 °C under an auto-generated pressure for 24 h in a 100 ml Teflon-lined autoclave. The $Na_2Ti_3O_7$ products were washed using distilled water and then soaked in diluted 0.2 M hydrochloric acid (HCl, 37%) for 4 h to obtain hydrogen titanate nanowires ($H_2Ti_3O_7$). Secondly, 0.150 g $H_2Ti_3O_7$ were

dispersed in 70 ml $Ba(OH)_2 \cdot 8H_2O$ solution (0.1 M) and the mixture was sonicated for 10 min. The hydrothermal reactions were carried out at 210 °C under auto-generated pressure for 24 h in a 100 ml Teflon-lined autoclave. The products were soaked in 0.2 M HCl solution briefly, then washed with distilled water several times and dried at 80 °C in an oven.

**2.2 Fabrication of $BaTiO_3$/P(VDF-CTFE) dielectric nanocomposites**

The anisotropic nanocomposites were fabricated using a deposition device based on a dispersing system (DR2203, EFD Inc., East Province, RI) according to our previous work.[44] 8 g of P(VDF-CTFE) (powder with 15% CTFE, PolyK Technologies, LLC, USA) was dissolved in 92 g dimethylformamide (DMF) and then was concentrated by evaporating the solvent to obtain high viscosity for printing. Samples with volume fractions of 2.5, 5.0 and 7.5% $BaTiO_3$ nanowires relative to the P(VDF-CTFE) were prepared. Figure 1a and 1b show optical photographs of the 3D printing equipment and a printed sample. The P(VDF-CTFE)/$BaTiO_3$/DMF mixtures were stirred and ultrasonically treated to form a uniform slurry. The slurry was transferred to an extrusion syringe with a nozzle of 100 μm diameter and pressure of 10-20 PSI. All of the samples were printed at room temperature on a three-axis CNC platform controlled by a computer regulator. The composites with randomly distributed $BaTiO_3$ nanowires were prepared by a casting method. $BaTiO_3$ nanowires were dispersed in 70 : 30 (volume fraction) acetone/DMF hybrid solvent with sonication and stirring, and then mixed with P(VDF-CTFE) powder for further stirring and sonication for 48 h. The suspension was cast onto the surface of a clean glass, and dried at 80 °C for 12

h at vacuum.

### 2.3 Characterization

The crystalline phases of $BaTiO_3$ nanowires were evaluated by X-ray powder diffraction (XRD, Rigaku D/max 2550, Japan) with Cu-Kα radiation (λ = 1.5418 Å) at room temperature. The morphology of the $BaTiO_3$ nanowires and nanocomposite films were observed using a scanning electron microscope (SEM, Nova NanoSEM230, USA). High-resolution transmission electron microscopy (HR-TEM) images of the $BaTiO_3$ nanowires were taken with a Titan G2 60-300, using an accelerating voltage of 300 kV. The morphology and orientation of the nanowire composites were examined using polarizing microscopy (POM, Leica DM-LM-P). The rheological properties of the $BaTiO_3$/PVDF-CTFE slurry were studied using a rotational rheometer (AR2000 EX, TA Instruments, New Castle, DE) with a parallel plate diameter of 40 mm. The frequency dependent permittivity and dielectric loss of the nanocomposite films were measured using an Agilent 4294A LCR meter with frequency ranging from 100 Hz to 10 MHz. The electric displacement-electric field (D-E) loops and leakage current were measured using a TF analyzer 2000 ferroelectric polarization tester (aixACT, Germany) and Delta 9023 furnace in a silicone oil bath at room temperature and 10 Hz.

## 3. Results and Discussion

Figures 1c and 1d show sketches of anisotropic nanocomposites with aligned $BaTiO_3$ nanowires induced by shear stress along the printing direction. During the extrusion process, the $BaTiO_3$ nanowires suffer from a high shear environment along the inner wall of the 100 μm diameter nozzle, which forces the $BaTiO_3$

nanowires to align parallel to the direction of printing.

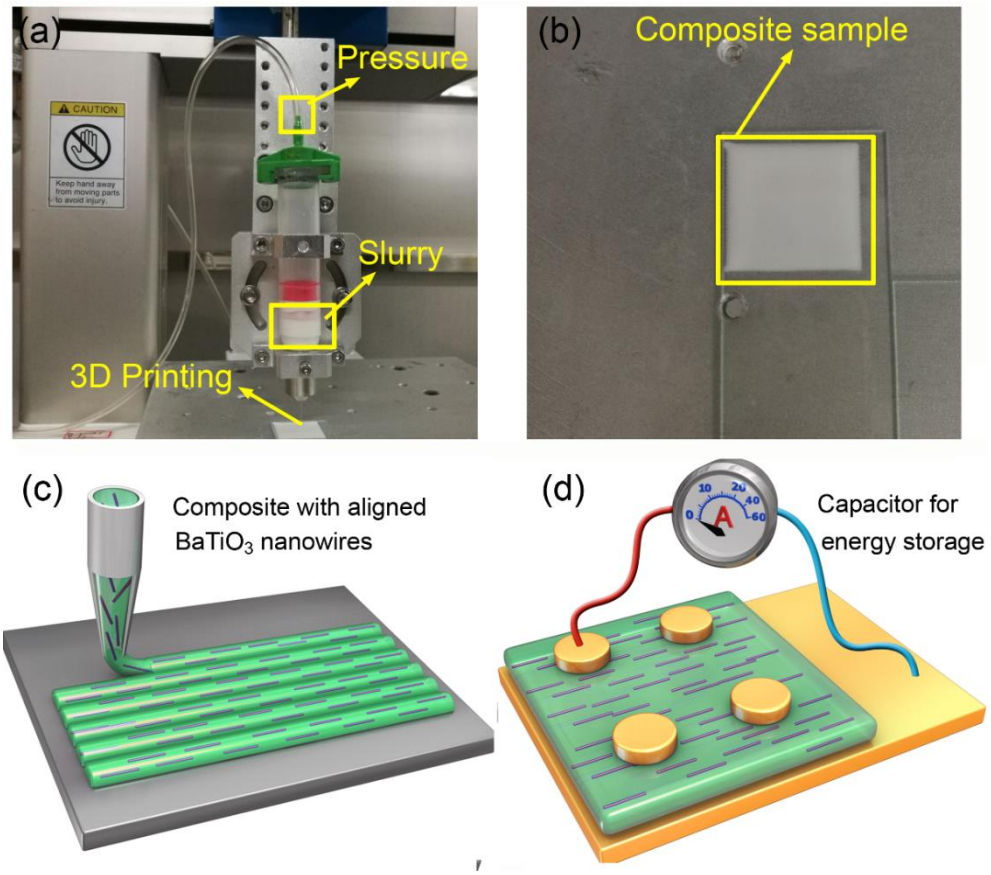


Figure 1. Alignment of $BaTiO_3$ nanowires in nanocomposites: photographs of (a) the printing assembly and (b) a printed nanocomposite sample; schematic illustrations of (c) the alignment of $BaTiO_3$ nanowires in the PVDF-CTFE matrix and (d) a nanocomposite capacitor for energy storage applications.

$BaTiO_3$ nanowires were selected as the fillers due to the advantages of high permittivity and low dielectric loss.[45-48] Firstly, high aspect ratio $Na_2Ti_3O_7$ nanowires with smooth surface were prepared, of which the morphologies and crystal structure were confirmed as shown in Figure S1a,b (Supporting Information). Then, the $Na_2Ti_3O_7$ nanowires were converted $H_2Ti_3O_7$ and finally to $BaTiO_3$ nanowires in the second step of the hydrothermal reaction. It is clear that the $BaTiO_3$ nanowires possess super-high aspect ratios and uniform morphology, as shown in Figure 2a and Figure S1c. Figure S1d shows the XRD pattern of $BaTiO_3$ nanowires, which can be attributed to the tetragonal phase of $BaTiO_3$ (PDF: 31-0174). Figure 2b shows a high

resolution transmission electron microscrograph of a single $BaTiO_3$ nanowire. Parallel lattice spacing of approximately 0.36 nm and 0.20 nm, corresponding to the (1-31) and (002) planes of the tetragonal phase, respectively were identified. The distribution of $BaTiO_3$ nanowire fillers in the nanocomposites is seen in the SEM and POM images shown Figures 1c and 1d, respectively. It is clear that the $BaTiO_3$ nanowires are well dispersed and aligned in one direction in the nanocomposite. For comparision, the SEM and POM images of the nanocomposites with randomly distributed $BaTiO_3$ nanowires prepared by the casting method are shown Figure S2e, f and Figure S3b.

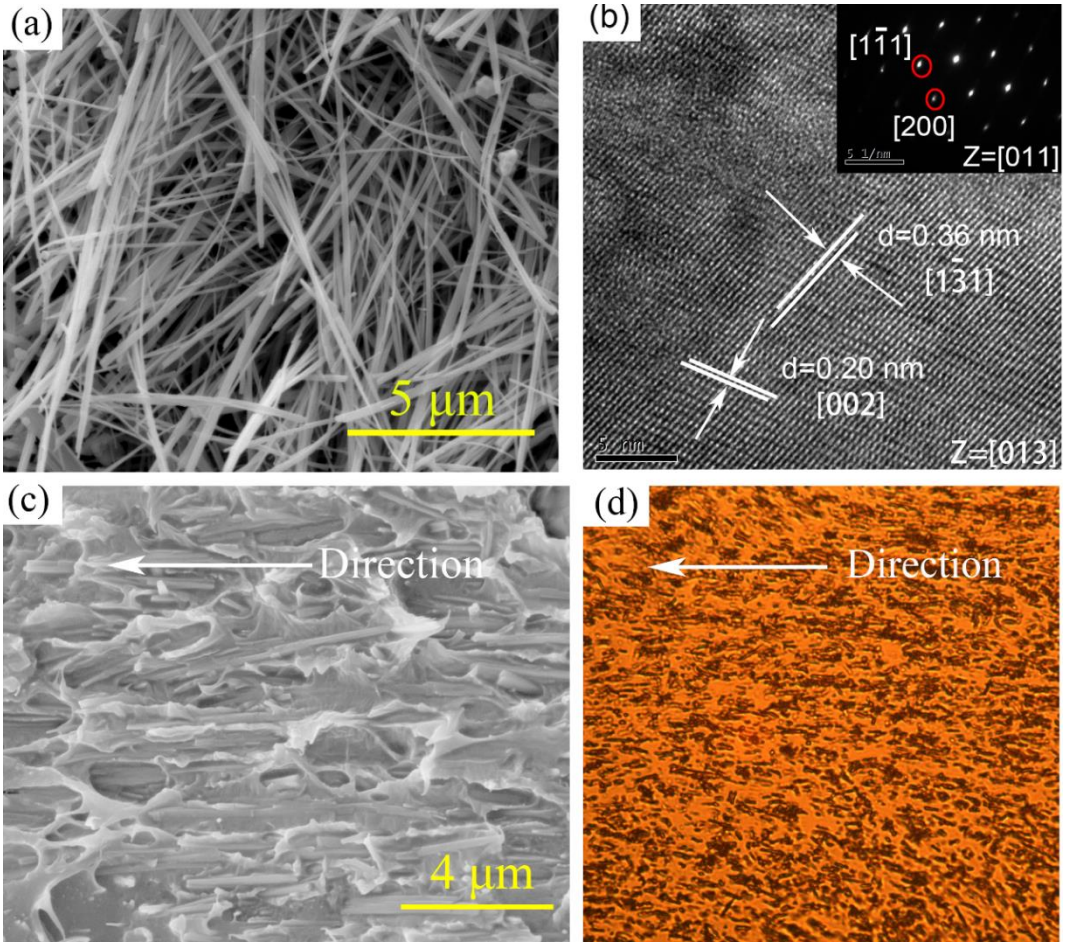


Figure 2 (a) SEM image of $BaTiO_3$ nanowires; (b) HRTEM image of a single $BaTiO_3$ nanowire; (c) SEM and (d) POM images of nanocomposites prepared by 3D printing with 5 vol% aligned $BaTiO_3$ nanowires.

Figure 3a shows the relationship between shear rate and viscosity in P(VDF-CTFE)

slurries with different volume fractions of $BaTiO_3$ nanowires. The slurries show shear thinning characteristics at low shear rate, and when the shear rate increases to around 100 $s^{-1}$, the viscosity of slurries is close to a constant value. At the shear rate of 100 $s^{-1}$, the viscosities of the three samples are about 6.7 mPa·s, which means that the change of filler loadings over a very small range shows little effect on the viscosity of the slurry. Figure 3b shows the shear rate dependent shear stress of slurries with different $BaTiO_3$ nanowires loadings. The slope of the curves represents the viscosity of the suspension. At a constant shear rate, the slurries shows similar viscosity, which is consistent with the results shown in Figure 3a. Slurries with shear thinning behavior meet the rheological requirements for application in 3D direct writing. At low shear rate, the slurries shows high viscosity, which allow them to avoid agglomeration and settling of the $BaTiO_3$ nanowires within the printing needle tube. At high shear rate, the slurries show low viscosity, which allows them to have sufficient fluidity to be extruded from the printing needle.[49, 50]

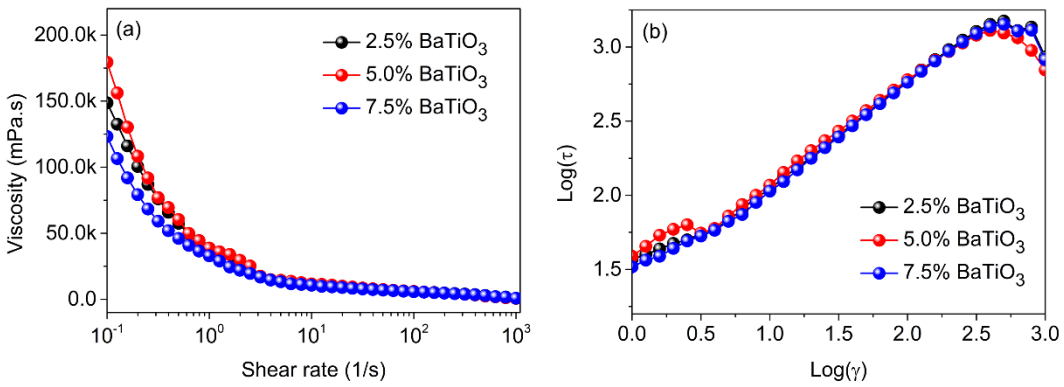


Figure 3 (a) Shear rate dependence of viscosity and (b) logarithmic plot of shear stress of the slurries with various $BaTiO_3$ loadings

Nanocomposites with different $BaTiO_3$ nanowire loadings were prepared by the 3D

direct writing method and compared with those made using a traditional solution casting method. The permittivity and dielectric loss of the prepared nanocomposites are summarized in Figure 4. Figure 4a and 4c shows the frequency dependent permittivity of $BaTiO_3$ nanowire/P(VDF-CTFE) nanocomposites, where the $BaTiO_3$ nanowires were aligned perpendicular to electric field direction (Figure 4a) compared to the random distribution (Figure 4c). The permittivity of the nanocomposites with aligned $BaTiO_3$ nanowires is smaller than that of nanocomposites with random $BaTiO_3$ nanowires. For example, when the loadings of random $BaTiO_3$ nanowires is 2.5, 5.0 and 7.5 vol%, the permittivity of the nanocomposites with random $BaTiO_3$ nanowires is 14, 15.5 and 21.5, respectively, while the permittivity of the nanocomposites with aligned $BaTiO_3$ nanowires is 12, 14 and 17.5, respectively (Fig 4d).

The total permittivity over the high and low frequency ranges ε′ is sum of interfacial and space charge contributions:

$$\varepsilon' = \varepsilon'_{MWS} + \varepsilon'_{DIP} \quad (1)$$

where，$\varepsilon'_{MWS}$ and $\varepsilon'_{DIP}$ represent interfacial polarization (in the low frequency range) and space charge polarization (in the high frequency range). Polarization (P) can be calculated using equation (2)：

$$P = \frac{\sum \mu}{V} = \frac{\sum ql}{V} \quad (2)$$

Where $q$, $l$, and $V$ are charge, distance between positive and negative charges and volume of the sample. When the ceramic fillers are distributed parallel to the electric field direction, $l$ is equal to the length of the ceramic nanowires (~several microns). When the ceramic fillers are distributed perpendicular to the electric field, $l$ is equal to

the diameter of the ceramic nanowires (~100 nm). This results in lower permittivity of nanocomposites with aligned $BaTiO_3$ nanowires compared to that of nanocomposites with randomly distributed $BaTiO_3$ nanowires.[32, 36]

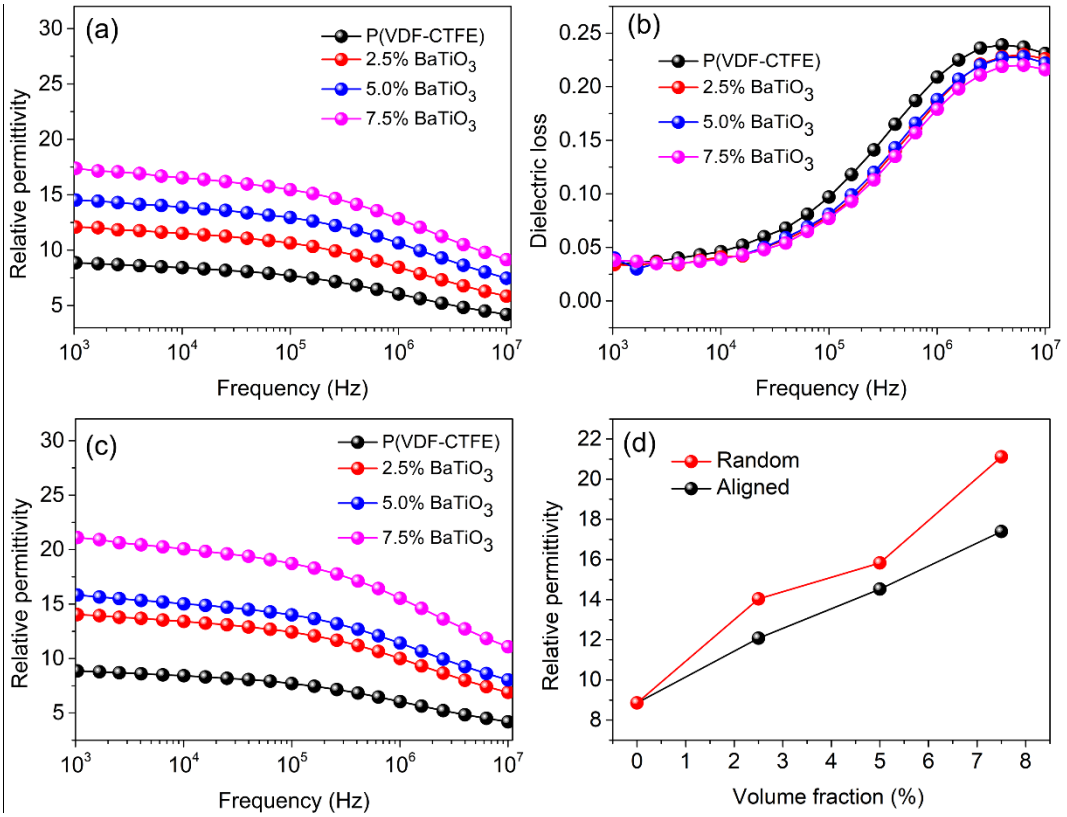


Figure 4 Frequency dependence of (a) relative dielectric permittivity and (b) dielectric loss of $BaTiO_3$/P(VDF-CTFE) nanocomposites with aligned $BaTiO_3$ nanowires, (c) relative dielectric permittivity of nanocomposites with random distributed $BaTiO_3$ nanowires; (d) relative dielectric permittivity of the nanocomposites as a function of volume fraction at 1 kHz

Figure 5a shows typical *P-E* loops for P(VDF-CTFE) nanocomposites with aligned $BaTiO_3$ nanowires, from which the saturation polarization and residual polarization can be obtained and the energy density can be calculated. Due to the high permittivity of $BaTiO_3$ fillers and the introduction of interfacial polarization, the saturation polarization increases with increasing $BaTiO_3$ loading. When the loading of aligned $BaTiO_3$ nanowires is 2.5 vol%, the nanocomposites achieve higher polarization and

breakdown strength (Figure S4) than that in P(VDF-CTFE). This means that nanocomposites with low loadings of aligned $BaTiO_3$ nanowires can simultaneous improve permittivity and breakdown strength. Figure 5b shows the characteristic breakdown strengths of nanocomposites with aligned and random $BaTiO_3$ nanowires at 5% loading. The nanocomposite with aligned $BaTiO_3$ nanowires possesses higher breakdown strength than the nanocomposite with random $BaTiO_3$ nanowires at the same loading level. The discharged energy density of the nanocomposites with aligned $BaTiO_3$ nanowires as a function of applied electric field is shown in Figure 5c. The discharged energy density of all composites is similar at low field, but at high field increases with increasing loading level. The maximum energy density achieved in nanocomposites with aligned $BaTiO_3$ nanowires was 14.52 J $cm^{-3}$ for the sample with 5.0 vol% loading, which is 55% higher than that of the nanocomposite with randomly aligned $BaTiO_3$ nanowires at the same loading level.

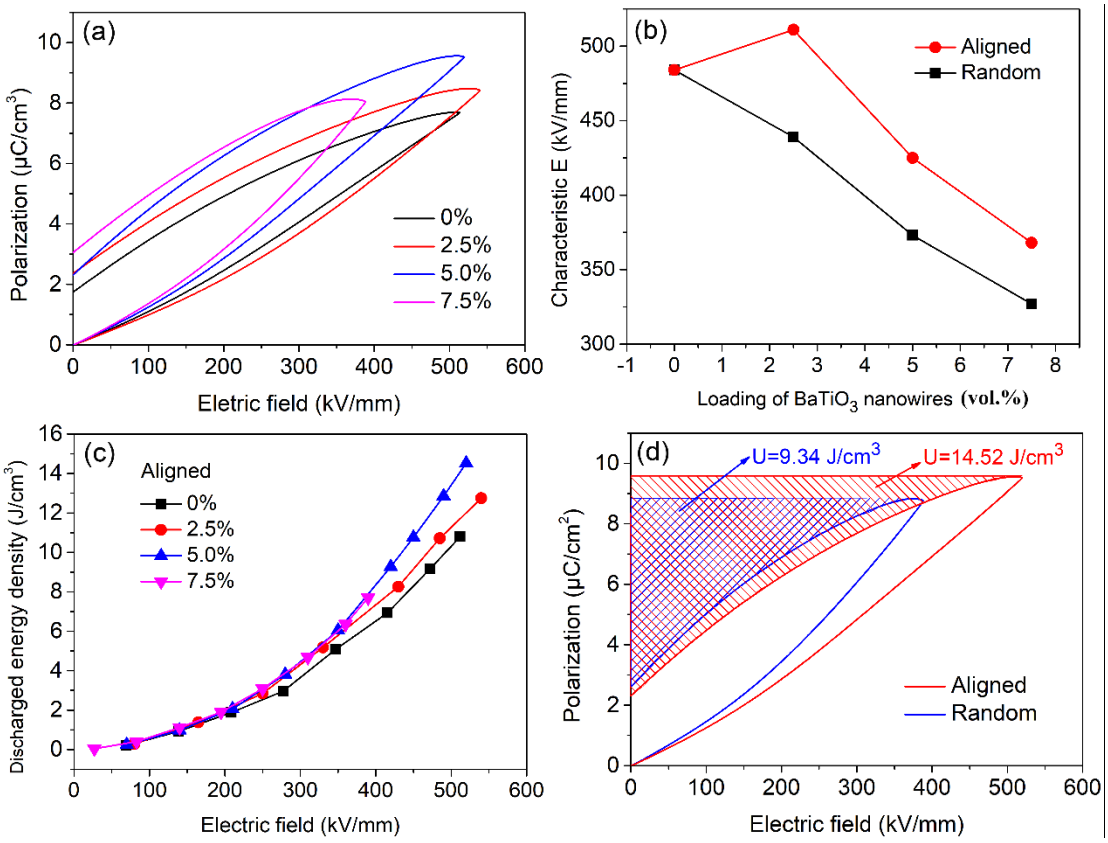


Figure 5 (a) *P-E* loops and (c) discharge energy density of P(VDF-CTFE) nanocomposites filled with aligned $BaTiO_3$ nanowires; (b) breakdown strength of P(VDF-CTFE) nanocomposites as a function of $BaTiO_3$ loading; (d) comparison of maximum discharged energy density and *P-E* loops of P(VDF-CTFE) nanocomposites with 5.0 vol% aligned and randomly distributed $BaTiO_3$ nanowires

## Conclusions

It has been shown that 3D printing is an effective method to prepare aligned $BaTiO_3$ nanowires/P(VDF-CTFE) nanocomposites. P(VDF-CTFE) nanocomposites with aligned $BaTiO_3$ nanowires possess higher breakdown strength and energy density compared to those with randomly distributed $BaTiO_3$ nanowires, with a maximum discharged energy density of 14.52 J/cm$^3$ achieved with 5.0 vol% nanowire loading, 55.5% higher than that of nanocomposites with randomly distributed nanowires at the same loading level. This work provides a facile route to align one dimensional

inorganic fillers in a polymer matrix that is readily scalable to prepare high performance dielectrics for capacitors.

## Acknowledgements

The authors would like to acknowledge funding from National Natural Science Foundation of China (51672311), Hunan Natural Science Foundation (2019JJ40349), China Postdoctoral Science Foundation (2017M620353), Special Funding for the Postdoctoral Science Fund of China (2018T110840), and State Key Laboratory of Powder Metallurgy, Central South University, Changsha, China.

**References**

[1] Meng N, Ren X, Santagiuliana G, Ventura L, Zhang H, Wu J, et al. Ultrahigh β-phase content poly(vinylidene fluoride) with relaxor-like ferroelectricity for high energy density capacitors. Nature Communications. 2019;10(1):4535.
[2] Guo M, Jiang J, Shen Z, Lin Y, Nan C-W, Shen Y. High-Energy-Density Ferroelectric Polymer Nanocomposites for Capacitive Energy Storage: Enhanced Breakdown Strength and Improved Discharge Efficiency. Materials Today. 2019;29:49-67.
[3] Huang X, Sun B, Zhu Y, Li S, Jiang P. High-k polymer nanocomposites with 1D filler for dielectric and energy storage applications. Progress in Materials Science. 2019;100:187-225.
[4] Zhu Y, Zhu Y, Huang X, Chen J, Li Q, He J, et al. High Energy Density Polymer Dielectrics Interlayered by Assembled Boron Nitride Nanosheets. Adv Energy Mater. 2019.
[5] Li Q, Chen L, Gadinski MR, Zhang S, Zhang G, Li H, et al. Flexible high-temperature dielectric materials from polymer nanocomposites. Nature. 2015;523(7562):576-+.
[6] Zhang X, Li B-W, Dong L, Liu H, Chen W, Shen Y, et al. Superior Energy Storage Performances of Polymer Nanocomposites via Modification of Filler/Polymer Interfaces. Advanced Materials Interfaces. 2018;5(11).
[7] Pan Z, Yao L, Zhai J, Yao X, Chen H. Interfacial Coupling Effect in Organic/Inorganic Nanocomposites with High Energy Density. Adv Mater. 2018;30(17).
[8] Luo H, Zhou X, Ellingford C, Zhang Y, Chen S, Zhou K, et al. Interface design for high energy density polymer nanocomposites. Chemical Society reviews. 2019;48(16):4424-65.

[9] Mannodi-Kanakkithodi A, Treich GM, Huan TD, Ma R, Tefferi M, Cao Y, et al. Rational Co-Design of Polymer Dielectrics for Energy Storage. Adv Mater. 2016;28(30):6277-91.
[10] Dang ZM, Yuan JK, Yao SH, Liao RJ. Flexible nanodielectric materials with high permittivity for power energy storage. Adv Mater. 2013;25(44):6334-65.
[11] Dang Z-M, Zheng M-S, Zha J-W. 1D/2D Carbon Nanomaterial-Polymer Dielectric Composites with High Permittivity for Power Energy Storage Applications. Small. 2016;12(13):1688-701.
[12] Wang G, Huang X, Jiang P. Tailoring Dielectric Properties and Energy Density of Ferroelectric Polymer Nanocomposites by High-k Nanowires. ACS Appl Mater Interfaces. 2015;7(32):18017-27.
[13] Wang Y, Wang L, Yuan Q, Chen J, Niu Y, Xu X, et al. Ultrahigh energy density and greatly enhanced discharged efficiency of sandwich-structured polymer nanocomposites with optimized spatial organization. Nano Energy. 2018;44:364-70.
[14] Meereboer NL, Terzic I, Portale G, Loos K. Improved energy density and charge-discharge efficiency in solution processed highly defined ferroelectric block copolymer-based dielectric nanocomposites. Nano Energy. 2019;64.
[15] Wang Y, Wang L, Yuan Q, Niu Y, Chen J, Wang Q, et al. Ultrahigh electric displacement and energy density in gradient layer-structured BaTiO3/PVDF nanocomposites with an interfacial barrier effect. J Mater Chem A. 2017;5(22):10849-55.
[16] Bi K, Bi M, Hao Y, Luo W, Cai Z, Wang X, et al. Ultrafine core-shell BaTiO3@SiO2 structures for nanocomposite capacitors with high energy density. Nano Energy. 2018;51:513-23.
[17] Yao Z, Song Z, Hao H, Yu Z, Cao M, Zhang S, et al. Homogeneous/Inhomogeneous-Structured Dielectrics and their Energy-Storage Performances. Adv Mater. 2017;29(20).
[18] Tang H, Lin Y, Sodano HA. Synthesis of High Aspect Ratio BaTiO3 Nanowires for High Energy Density Nanocomposite Capacitors. Adv Energy Mater. 2013;3(4):451-6.
[19] Kim P, Doss NM, Tillotson JP, Hotchkiss PJ, Pan M-J, Marder SR, et al. High energy density nanocomposites based on surface-modified $BaTiO_3$ and a ferroelectric polymer. ACS Nano. 2009;3(9):2581-92.
[20] Tang H, Sodano HA. Ultra High Energy Density Nanocomposite Capacitors with Fast Discharge Using $Ba_{0.2}Sr_{0.8}TiO_3$ Nanowires. Nano Lett. 2013;13(4):1373-9.
[21] Tang H, Lin Y, Sodano HA. Enhanced Energy Storage in Nanocomposite Capacitors Through Aligned PZT Nanowires by Uniaxial Strain Assembly. Adv Energy Mater. 2012;2(4):469-76.
[22] Zhang D, Ma C, Zhou X, Chen S, Luo H, Bowen CR, et al. High Performance Capacitors Using BaTiO3 Nanowires Engineered by Rigid Liquid-crystalline Polymers. The Journal of Physical Chemistry C. 2017;121(37):20075-83.
[23] Zhang D, Zhou X, Roscow J, Zhou K, Wang L, Luo H, et al. Significantly Enhanced Energy Storage Density by Modulating the Aspect Ratio of BaTiO3 Nanofibers. Scientific Reports. 2017;7:45179.

[24] Luo H, Chen S, Liu L, Zhou X, Ma C, Liu W, et al. Core–Shell Nanostructure Design in Polymer Nanocomposite Capacitors for Energy Storage Applications. ACS Sustainable Chemistry & Engineering. 2018.
[25] Luo H, Roscow J, Zhou X, Chen S, Han X, Zhou K, et al. Ultra-high discharged energy density capacitor using high aspect ratio Na 0.5 Bi 0.5 TiO 3 nanofibers. J Mater Chem A. 2017;5(15):7091-102.
[26] Zhang D, Liu W, Guo R, Zhou K, Luo H. High Discharge Energy Density at Low Electric Field Using an Aligned Titanium Dioxide/Lead Zirconate Titanate Nanowire Array. Advanced Science. 2017:1700512.
[27] Zhang D, Liu W, Tang L, Zhou K, Luo H. High performance capacitors via aligned TiO2 nanowire array. Appl Phys Lett. 2017;110(13):133902.
[28] Luo H, Ma C, Zhou X, Chen S, Zhang D. Interfacial Design in Dielectric Nanocomposite Using Liquid-Crystalline Polymers. Macromolecules. 2017;50(13):5132-7.
[29] Li J, Khanchaitit P, Han K, Wang Q. New route toward high-energy-density nanocomposites based on chain-end functionalized ferroelectric polymers. Chem Mater. 2010;22(18):5350-7.
[30] Kim T, Trangkanukulkij R, Kim WS. Nozzle Shape Guided Filler Orientation in 3D Printed Photo-curable Nanocomposites. Scientific Reports. 2018;8(1):3805.
[31] Hu N, Karube Y, Yan C, Masuda Z, Fukunaga H. Tunneling effect in a polymer/carbon nanotube nanocomposite strain sensor. Acta Materialia. 2008;56(13):2929-36.
[32] Zhong S-L, Yin L-J, Pei J-Y, Li X-Y, Wang S-J, Dang Z-M. Effect of fiber alignment on dielectric response in the 1-3 connectivity fiber/polymer composites by quantitative evaluation. Appl Phys Lett. 2018;113(12).
[33] Andrews C, Lin Y, Sodano HA. The effect of particle aspect ratio on the electroelastic properties of piezoelectric nanocomposites. Smart Materials & Structures. 2010;19(2).
[34] Xie B, Zhang H, Zhang Q, Zang J, Yang C, Wang Q, et al. Enhanced energy density of polymer nanocomposites at a low electric field through aligned BaTiO3 nanowires. J Mater Chem A. 2017;5(13):6070-8.
[35] Zhang X, Jiang J, Shen Z, Dan Z, Li M, Lin Y, et al. Polymer Nanocomposites with Ultrahigh Energy Density and High Discharge Efficiency by Modulating their Nanostructures in Three Dimensions. Adv Mater. 2018;30(16).
[36] He D, Wang Y, Song S, Liu S, Deng Y. Significantly Enhanced Dielectric Performances and High Thermal Conductivity in Poly(vinylidene fluoride)-Based Composites Enabled by SiC@SiO2 Core-Shell Whiskers Alignment. ACS Appl Mater Interfaces. 2017;9(51):44839-46.
[37] Gao M, Li L, Li W, Zhou H, Song Y. Direct Writing of Patterned, Lead-Free Nanowire Aligned Flexible Piezoelectric Device. Advanced Science. 2016;3(8):n/a-n/a.
[38] Kim JH, Lee S, Wajahat M, Jeong H, Chang WS, Jeong HJ, et al. Three-Dimensional Printing of Highly Conductive Carbon Nanotube Microarchitectures with Fluid Ink. ACS Nano. 2016;10(9):8879.

[39] Compton BG, Lewis JA. 3D-printing of lightweight cellular composites. Adv Mater. 2015;26(34):5930-5.
[40] Yunus DE, Shi W, Sohrabi S, Liu Y. Shear induced alignment of short nanofibers in 3D printed polymer composites. Nanotechnology. 2016;27(49).
[41] Phatharapeetranun N, Ksapabutr B, Marani D, Bowen JR, Esposito V. 3D-printed barium titanate/poly-(vinylidene fluoride) nano-hybrids with anisotropic dielectric properties. J Mater Chem C. 2017;5.
[42] Kanguk K, Wei Z, Xin Q, Chase A, Mccall WR, Shaochen C, et al. 3D optical printing of piezoelectric nanoparticle-polymer composite materials. ACS Nano. 2014;8(10):9799.
[43] Xie B, Zhang Q, Zhang H, Zhang G, Qiu S, Jiang S. Largely enhanced ferroelectric and energy storage performances of P (VDF-CTFE) nanocomposites at a lower electric field using BaTiO3 nanowires by stirring hydrothermal method. Ceramics International. 2016;42(16):19012-8.
[44] Liao J, Chen H, Hang L, Wang X, Zhou K, Dou Z. Direct Ink Writing of Zirconia Three-Dimensional Structures. J Mater Chem C. 2017;5(24).
[45] Jiang B, Iocozzia J, Zhao L, Zhang H, Harn Y-W, Chen Y, et al. Barium titanate at the nanoscale: controlled synthesis and dielectric and ferroelectric properties. Chemical Society Reviews. 2019;48(4):1194-228.
[46] Xu W, Yang G, Jin L, Liu J, Zhang Y, Zhang Z, et al. High-k Polymer Nanocomposites Filled with Hyperbranched Phthalocyanine-Coated BaTiO3 for High-Temperature and Elevated Field Applications. ACS Appl Mater Interfaces. 2018;10(13):11233-41.
[47] Hu P, Gao S, Zhang Y, Zhang L, Wang C. Surface modified BaTiO3 nanoparticles by titanate coupling agent induce significantly enhanced breakdown strength and larger energy density in PVDF nanocomposite. Composites Science and Technology. 2018;156:109-16.
[48] Hao YN, Wang XH, O'Brien S, Lombardi J, Li LT. Flexible BaTiO3/PVDF gradated multilayer nanocomposite film with enhanced dielectric strength and high energy density. J Mater Chem C. 2015;3(37):9740-7.
[49] Phatharapeetranun N, Ksapabutr B, Marani D, Bowen JR, Esposito V. 3D-printed barium titanate/poly-(vinylidene fluoride) nano-hybrids with anisotropic dielectric properties. J Mater Chem C. 2017;5(47):12430-40.
[50] Gao M, Li L, Li W, Zhou H, Song Y. Direct Writing of Patterned, Lead-Free Nanowire Aligned Flexible Piezoelectric Device. Advanced Science. 2016;3(8).

# 3D Printing of Anisotropic Polymer Nanocomposites with Aligned $BaTiO_3$ Nanowires for Enhanced Energy Density

Hang Luo[a], Xuefan Zhou[a], Ru Guo[a], Xi Yuan[a]*, Hehao Chen[a], Kechao Zhou[a], Isaac Abrahams[b], Dou Zhang[a]*

[a] State Key Laboratory of Powder Metallurgy, Central South University, Changsha, Hunan 410083, China

[b] Materials Research Institute, School of Biological Sciences, Queen Mary University of London, Mile End Road, London E1 4NS, UK

The Email of the corresponding author:

dzhang@csu.edu.cn (D. Zhang)

yuanxi0731@163.com (X. Yuan)

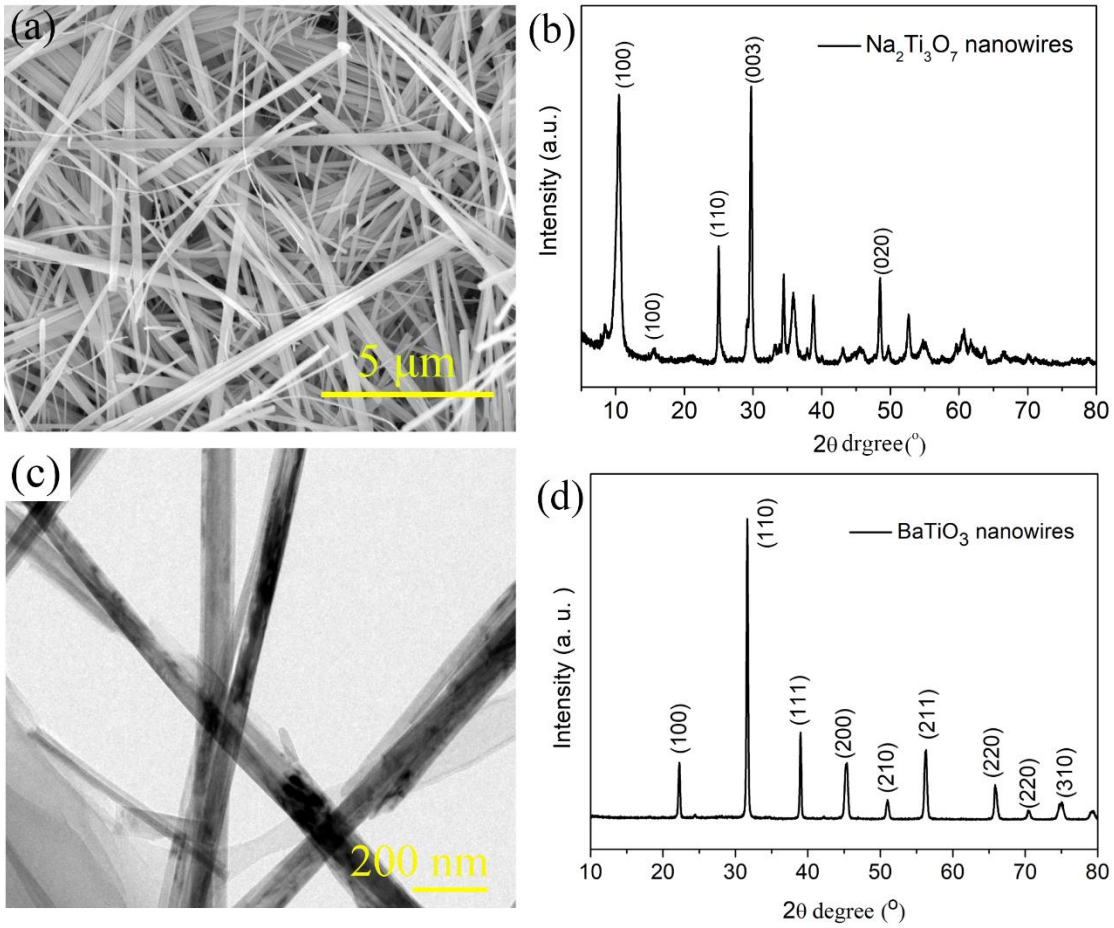


Figure S1 (a) SEM image and (b) XRD pattern of $Na_2Ti_3O_7$ nanowires; (c) TEM image and (d) XRD pattern of $BaTiO_3$ nanowires

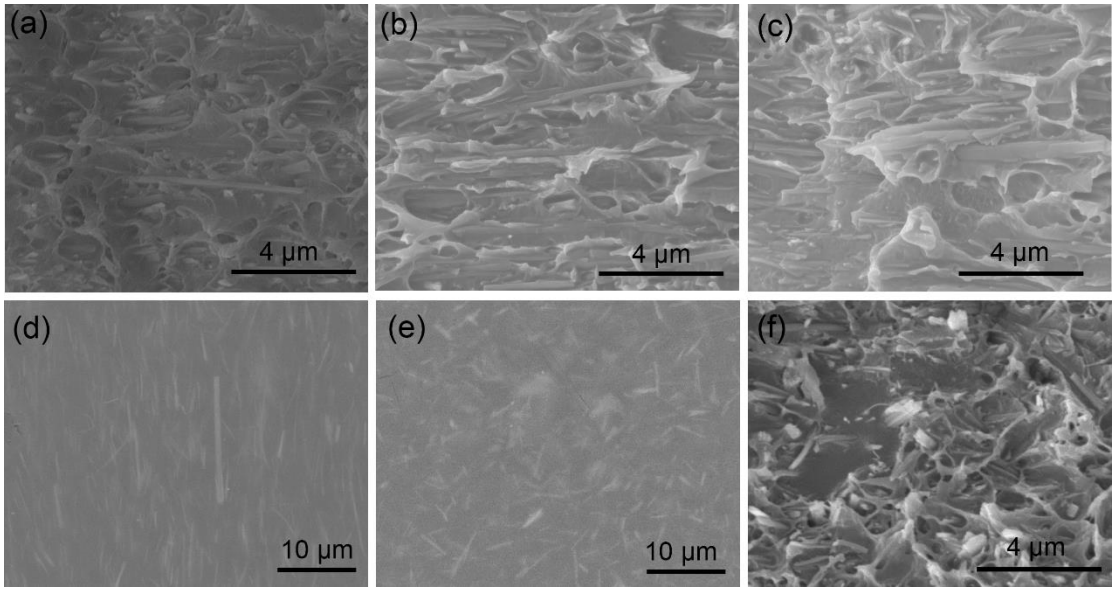


Figure S2 Scanning Electron Microscope (SEM) images of cross-sections of P(VDF-CTFE) nanocomposites with (a) 2.5vol.%, (b) 5.0 vol.%, and (c) 7.5 vol.% aligned $BaTiO_3$ nanowires, (d) top-surface SEM images of the P(VDF-CTFE) nanocomposites with 5.0 vol.% aligned $BaTiO_3$ nanowires; For comparison, (e) top-surface (f) cross-section SEM images of P(VDF-CTFE) nanocomposites with 5.0 vol.% randomly distributed $BaTiO_3$ nanowires.

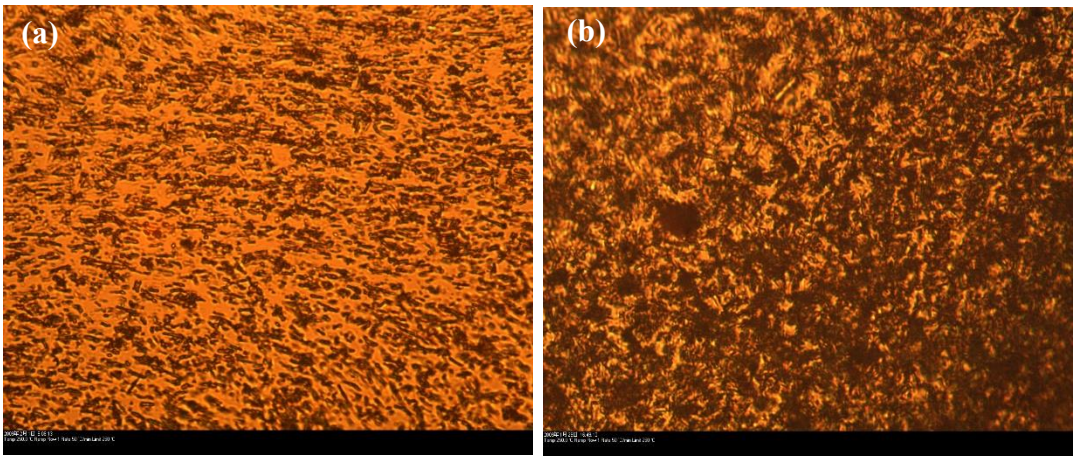


Figure S3 Polarizing microscope (POM) images of the nanocomposites with 5 vol.% (a) aligned, and (b) randomly distributed $BaTiO_3$ nanowires.

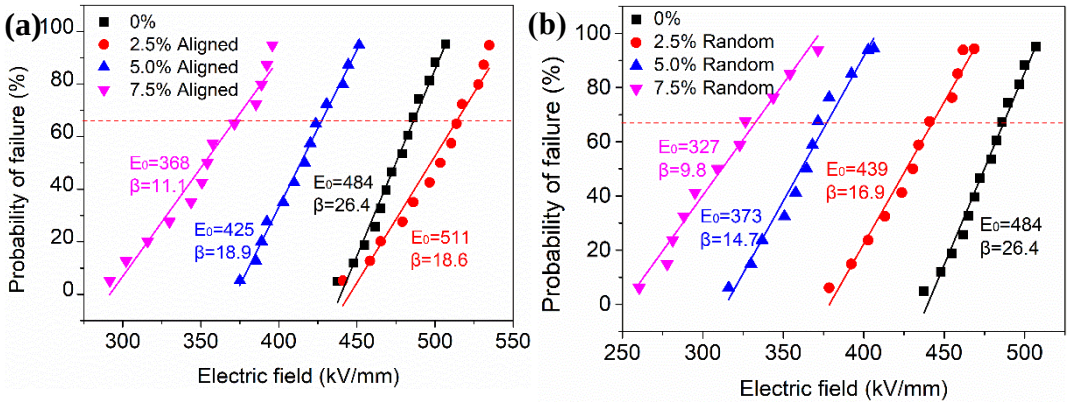


Figure S4 Weibull distributions of the dielectric breakdown strength of P(VDF-CTFE) nanocomposites filled with (a) aligned and (b) randomly distributed $BaTiO_3$ nanowires.